journal

J. Am. Ceram. Soc., 79 [1] 233–38 (1996)

Superplastic Alumina at Temperatures below 1300°C Using Charge-Compensating Dopants

Liang A. Xue*,† and I-Wei Chen*

Department of Materials Science and Engineering, University of Michigan, Ann Arbor, Michigan 48109-2136

To achieve low-temperature superplasticity in alumina, we have introduced charge-compensating dopants, Ti^{4+} and Mn^{2+}, which jointly have a high solubility and significantly enhance the diffusion and deformation processes during sintering and forming. Zirconia as a second-phase pinning agent has also been incorporated to impart microstructural stability against static and dynamic grain growth. The superplastic alumina obtained can be shape-formed under biaxial tension to 100% engineering strain at temperatures below 1300°C. Deformation characteristics of this alumina at temperatures from 1200° to 1400°C and at strain rates from 4×10^{-6} to 3×10^{-3}/s are described. The origin of enhanced kinetics is attributed to the formation and dissociation of dopant-defect complexes.

I. Introduction

THE constitutive equation of superplastic deformation can be expressed in the following form:[1]

$$\dot{\varepsilon} = A\sigma^n/d^p \quad (1)$$

where $\dot{\varepsilon}$ is the strain rate, σ is the stress, d is the grain size, n and p are stress and grain size exponents, respectively, and A is a temperature-dependent, diffusion-related coefficient. For superplastic ceramics, n and p are typically between 1 and 3. The above constitutive equation suggests two basic approaches to promote superplastic deformation:[2] (1) obtaining a fine-grained microstructure which is stable against coarsening during sintering and deformation, and (2) enhancing lattice diffusivity, grain boundary diffusivity, or introducing a grain boundary liquid phase as a fast diffusion path.

Grain size control can be achieved through low-temperature sintering and the use of additives. In the case of alumina, this approach has been successfully applied to achieve superplasticity.[3] The additives used were MgO and ZrO_2 to take advantage of the solute segregation effect of Mg ions and the particle pinning effect of ZrO_2. These materials can be superplastically deformed in biaxial tension to 100% engineering strain at 1450°C.[3]

The utility of the second approach to achieve superplasticity in alumina, however, remains to be demonstrated. On one hand, although a grain boundary liquid phase serves to greatly enhance the deformation rate in compression, the tensile ductility was found to be low because of anisotropic grain growth and the degradation of grain boundary strength.[2,4] On the other hand, while MgO was found to have a relatively small enhancing effect on lattice diffusivity and to have little or a small depressing effect on grain boundary diffusivity,[5–7] ZrO_2 was reported to severely lower the deformation rate of alumina.[2,3,8]

Other aliovalent dopants in solid solution have been known to increase the defect concentrations and hence the diffusivities. For example, Ti^{4+} (Refs. 9 and 10) and Mn^{2+} (Refs. 11 and 12) were found to promote alumina sintering through their effect on lattice diffusivities. Ti^{4+}, Fe^{2+}, and Mn^{2+} were also found to enhance creep of alumina.[13–15] The difficulty encountered here, though, is that for alumina, a highly stoichiometric ceramic, the solubilities of aliovalent dopants are rather low, usually in the hundred ppm range. This is especially true for fixed valence cations such as Mg^{2+} and Zr^{4+}; but even for mixed valence cations such as Ti, Fe, and Mn, the solubility is still severely limited. This, in turn, limits the extent of the additive effect.

Codoping of charge-compensating dopants has been known to greatly increase the solubility of both ions[15] and significantly enhance sintering and creep of alumina.[16–20] Although previous deformation studies on such alumina achieved only a relatively low strain rate, $<10^{-5}$/s, due to the coarse-grained (on the order of 10 μm) samples used,[18–20] this approach seems promising enough to warrant further exploitation. In the present paper, we show that by the codoping of charge-compensating dopants, namely, $Ti^{4+} + Mn^{2+}$, and by reducing the grain size, diffusion/deformation processes of alumina during sintering/superplastic forming can be significantly enhanced to achieve superplasticity at temperatures as low as 1280°C. This demonstrates the utility of the second approach using aliovalent dopants to promote ceramic superplasticity. Simultaneously, noting that the defect chemistry of charge-compensating doping has hardly been discussed in the literature despite its known effect on creep and sintering, we have also taken this opportunity to address the likely mechanisms of enhanced kinetics caused by charge-compensating dopants.

II. Experimental Procedure

Two alumina compositions were studied. The first one contains 1 mol% Ti^{4+} and 1 mol% Mn^{2+}, with additional minor dopants of 1000 ppm ZrO_2, 1000 ppm MgO, and 500 ppm Y_2O_3. The second composition was the same as the first one but with 3 mol% ZrO_2 instead. The addition of MgO and Y_2O_3 was to improve microstructural homogeneity and to retard grain growth.[6,21] The small addition of ZrO_2 in the first composition was to establish a base-line to account for the very pronounced hardening effect known for this system.[2,8] The addition of 3 mol% ZrO_2 was for particle pinning of the grain boundary. In the following, these two compositions will be referred to by their ZrO_2 concentration (0.1% and 3%).

The starting material was a high-purity (>99.99%) alumina powder (TM-D, Taimei Chemicals, Tokyo, Japan) with an average particle size of ~0.2 μm. The powder was dispersed in distilled water with a surfactant (Darvan 821A). Aqueous solutions of $Mn(NO_3)_2$, $Mg(NO_3)_2$, $Y(NO_3)_3$, and $ZrOCl_2$ were later added, followed by the addition of an ethanol solution of $Ti(C_4H_9O)_4$ (titanium butoxide). The pH of the mixture was then adjusted to flocculate the suspension, and the slurry was dried and calcined at 900°C for 1 h. The powder thus obtained was again dispersed in distilled water with the surfactant by

R. Raj—contributing editor

Manuscript No. 194294. Received August 23, 1993; approved July 21, 1995.
Supported by the U.S. National Science Foundation under Grant No. DDM-9024975.
*Member, American Ceramic Society.
†Present address: Research and Technology, Allied Signal, Inc., Morristown, New Jersey 07962.

attrition-milling in an alumina jar using alumina milling balls. The suspension was then cast, under a pressure of 1 MPa, into green cakes, which were dried first in air and subsequently in an oven at 130°C. After isostatic pressing, these cakes were sintered in air for 1 h at 1230°C for the first composition and 1250°C for the second composition. During the sample preparation, plastic ware was used throughout the wet processes to avoid contamination.

The density of the sintered materials was determined by water immersion. Specimens with greater than 98% of the theoretical density were used in the deformation study. Microstructures of the as-sintered and the deformed specimens were characterized by scanning electron microscopy (SEM). The grain size was obtained by multiplying the average linear intercept length of at least 400 grains by 1.56. For deformed specimens, measurements were taken at directions both parallel and perpendicular to the axis of the applied stress, and the average was used. X-ray diffraction (XRD) was employed to determine the phase assemblage. The distribution of Ti^{4+} and Mn^{2+} in the materials was analyzed by energy dispersive X-ray microanalysis (EDX) intensities.

Specimens for compression tests were square bars with an aspect ratio of 2.1. Deformation was conducted in uniaxial compression in air, between 1200° and 1350°C, with strain rates from 4×10^{-6} to 3×10^{-3}/s. Specimens for the punch stretching test[22] were circular disks of a thickness of 1.2 mm and a diameter of 28 mm. During the stretching, a disk was placed between a SiC hemispherical punch of 6.5 mm diameter and a graphite circular die. After heating to the desired temperature, the punch was advanced following a programmed displacement–time profile to deform the disk into a hat-shaped alumina article with a hemispherical dome. Other experimental details for compression testing and superplastic stretching were the same as reported previously.[22–24]

III. Results

(1) *Sintered Microstructures*

Compared with pure alumina,[18] the Ti-Mn codoping reduces the sintering temperature of the submicrometer-sized alumina powder by at least 50°C. SEM micrographs of polished and

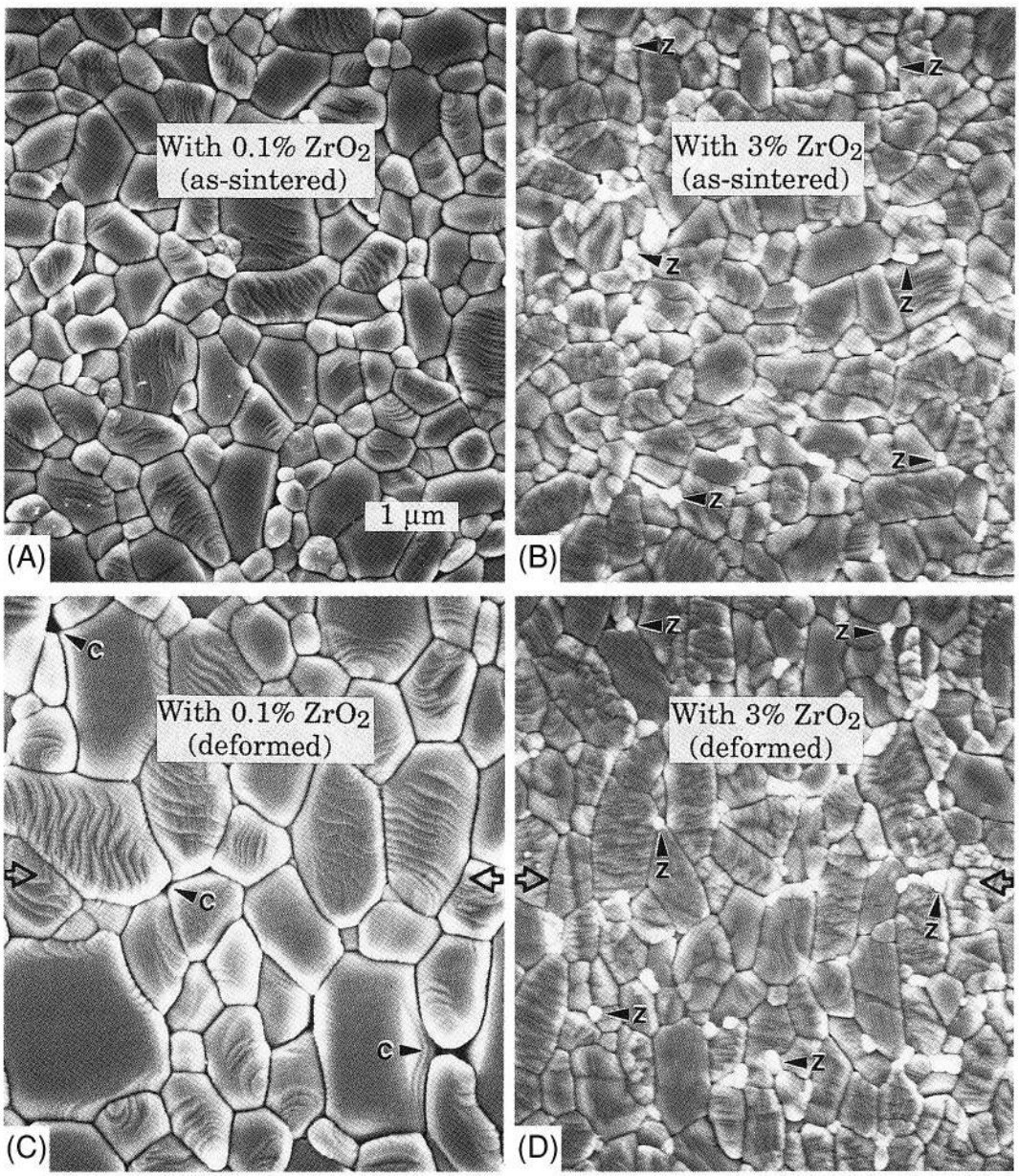

Fig. 1. SEM micrographs of Ti/Mn-doped alumina. As-sintered specimens with (A) 0.1% ZrO_2 and (B) 3% ZrO_2. Deformed specimens with (C) 0.1% ZrO_2, $\varepsilon = -0.53$ and (D) 3% ZrO_2, $\varepsilon = -0.64$. The compression axis is marked by hollow arrows in (C) and (D) and representative ZrO_2 particles in (B) and (D) are indicated by small solid arrows (z). Examples of cavities in (C) are also marked by small solid arrows (c).

thermally etched cross sections of as-sintered samples of the two alumina, with 0.1% and 3% ZrO_2 addition, are shown in Figs. 1(A) and (B). The 0.1%-ZrO_2-added alumina has an average grain size of 0.71 μm. The grain size distribution is relatively broad, which is characteristic of pure alumina.[23] No obvious second phase could be seen in this material on both the unetched and etched surfaces, using SEM with either secondary or backscattering electro-imaging. Thus, although second phases (zirconia, yttria, and spinel) were possibly present in this material, in view of the small solubilities for Zr, Y, and Mg, they were too small to be resolved by these techniques. The absence of detectable second phases was supported by XRD. In addition, EDX point analysis showed that Zr, Ti, and Mn concentrations were all below the instrument detectability throughout the specimens. The 3%-ZrO_2-added alumina shows a finer, more homogeneous microstructure, with an average alumina grain size of 0.66 μm. Some dispersed intergranular zirconia particles (white ones in Fig. 1(B)) were also visible. The zirconia phase was confirmed by XRD, which detected a predominantly tetragonal phase. The EDX results verified the presence of Zr in the white particles, with some Ti enrichment. The latter, along with other cations, is probably responsible for the stabilization of the tetragonal phase.[25]

(2) Deformation and Grain Growth

Stress (true) strain curves for the two alumina at 1300°C and at a constant strain rate of 3×10^{-4}/s in compression are shown in Fig. 2. Strain hardening is evident for both but especially pronounced for the 0.1%-ZrO_2-added material. The corresponding microstructures of these two specimens after deformation are given in Figs. 1(C) and (D). Some cavitation can be observed in the former (0.1% ZrO_2) but not in the latter (3% ZrO_2). Grain growth in the 0.1%-ZrO_2-added alumina is much more significant than that in the 3%-ZrO_2-added alumina. This apparently accounts for the different strain hardening behavior which, in turn, affects cavitation.[26] The grain growth was mainly induced by the deformation because statically annealed samples showed considerably less grain growth than the deformed ones. Similar observations on dynamic grain growth and the attendant strain hardening have been made for pure alumina,[23] for MgO-doped alumina,[23,27,28] and for MgO–Y_2O_3 or MgO–Cr_2O_3 codoped alumina.[21] The addition of 3% ZrO_2 effectively suppresses both static and dynamic grain growth.

The data of strain rate and flow stress at 1300°C for the two aluminas are compared on a logarithmic scale in Fig. 3. To reduce the influence of grain growth, flow stress at 3% strain was used here. It can be seen that the deformation behaviors of the two materials are almost identical. This is accidental, however, since there is a slight difference in grain size (0.71 μm for 0.1%-ZrO_2-added and 0.66 μm for 3%-ZrO_2-added alumina). Taking into account this difference and assuming $p = 2$, the 0.1%-ZrO_2-added alumina is estimated to have a normalized strain rate about 15% faster than that of the 3%-ZrO_2-added one. This could be due to the Ti enrichment in ZrO_2 particles which depletes the Ti concentration, and hence, its beneficial effect on deformation in the alumina (see below). Otherwise, because of the softening effect of ZrO_2,[3] 3%-ZrO_2-added alumina should have a higher normalized strain rate than 0.1%-ZrO_2-added alumina. (The latter, though, is harder than pure Al_2O_3, and hence, our choice as the base-line for comparison.[3])

For the 3%-ZrO_2-added alumina, the data for flow stress and strain rate at various deformation temperatures are plotted on the logarithmic scale in Fig. 4. Data for pure alumina[23] at 1350°C are also indicated (by the dashed line) for comparison. The strain rate of the Ti-Mn-doped alumina, with 3% ZrO_2, is ~40 times higher than that of pure alumina at 1350°C. This is despite the smaller grain size of the pure alumina (0.5 μm) according to Ref. 23. Taking this into account and assuming $p = 2$,[3] the codoping of Ti and Mn is estimated to enhance the deformation rate of alumina by a factor of about 70. Despite the large difference in strain rate, the stress exponent n of the doped alumina (1.6–1.7) is close to that of pure alumina (~1.7).[23] This value is within the range (1.5 to 2) reported in the literature for various fine-grained, pure or lightly doped, alumina.[8,29,30]

The temperature dependence of the strain rate for the 3%-ZrO_2-added alumina is shown in Fig. 5, where the strain rate at 40 MPa is plotted against reciprocal absolute temperature. The activation energy calculated from the slope is 728 kJ/mol. This value is much higher than that obtained for pure alumina (460 kJ/mol).[23] It is also beyond the range of the reported activation energy values in the literature for pure and lightly doped alumina (410–625 kJ/mol).[21,29,30] However, it has been reported that in alumina/zirconia composites (with 50–80% Al_2O_3) the deformation activation energy is as high as 750 kJ/mol, more than that of either alumina or zirconia.[31] Indeed, even the 0.1% ZrO_2 addition to Al_2O_3 can cause the same effect.[3,8] The present data are superficially consistent with these reports. The main difference, though, is that these previous reports of higher activation energies are associated with slower strain rates, whereas the present work demonstrates a faster strain rate despite a higher activation energy. Note that a similar report on a higher activation energy and a higher strain rate has also been made for Al_2O_3–TiO_2 two-phase materials in Refs. 9, 32, and 33. This aspect will be discussed later in conjunction with diffusion and defect mechanisms.

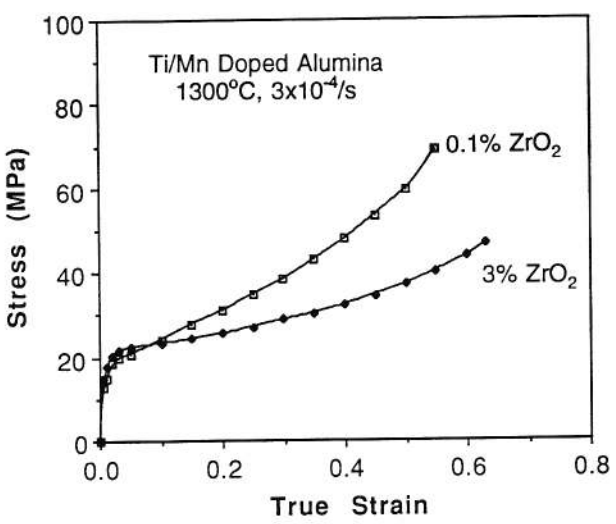

Fig. 2. Stress–strain curves at 1300°C, at a constant strain rate of 3×10^{-4}/s, for 0.1%-ZrO_2-added and 3%-ZrO_2-added Ti/Mn-doped alumina.

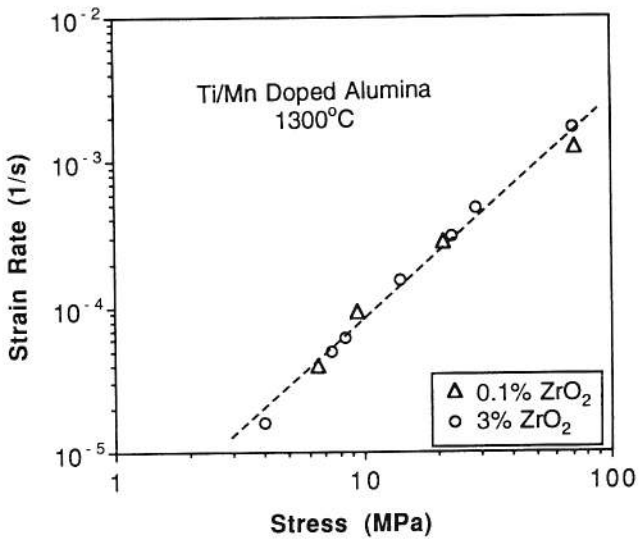

Fig. 3. Strain rate–stress relationships at 1300°C for 0.1%-ZrO_2-added and 3%-ZrO_2-added Ti/Mn-doped alumina.

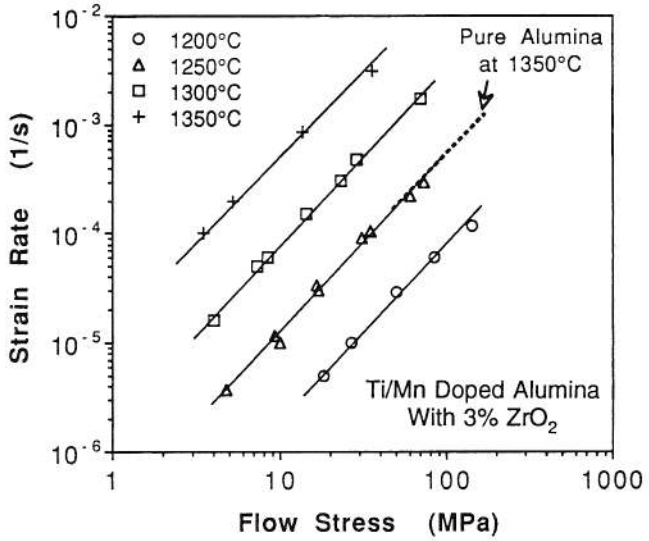

Fig. 4. Relationship between strain rate and flow stress at various temperatures for the Ti/Mn-doped alumina (0.66 μm) with 3% ZrO_2. The dashed line is for pure alumina (0.5 μm) at 1350°C from Ref. 23.

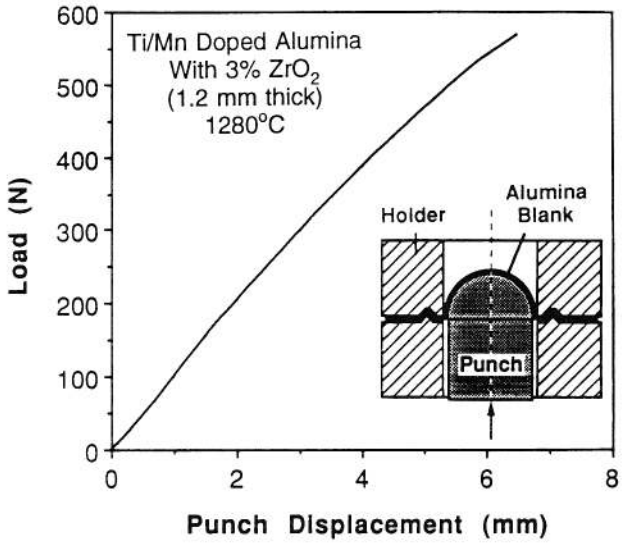

Fig. 6. Forming load versus punch displacement for the Ti/Mn-doped alumina with 3% ZrO_2 during superplastic stretching at 1280°C. The average strain rate was 2.3×10^{-4}/s.

(3) Superplastic Stretching

The superplastic formability of the 3-mol%-ZrO_2-added alumina was demonstrated by the punch stretching test described elsewhere.[22] In this test, a flat disk is stretched by a hemispherical punch to a dome shape. When the height of the dome reaches the same as the dome radius, the surface area is approximately twice that of the original, corresponding to a biaxial tensile engineering strain of 100%.

A typical forming curve of load versus punch displacement for the alumina at 1280°C is shown in Fig. 6. The punch radius used was 6.5 mm. The average strain rate in this test was 2.3×10^{-4}/s. The increase in load with the displacement is due mainly to the increase in the deforming area of the specimen, since grain growth/strain hardening is fairly modest in this alumina. The test was completed in 50 min, yielding a half-spherical-shaped dome with no obvious surface defects. At a slightly higher temperature of 1300°C, punch stretching was achieved at a higher average strain rate of 4×10^{-4}/s and completed in less than 30 min.

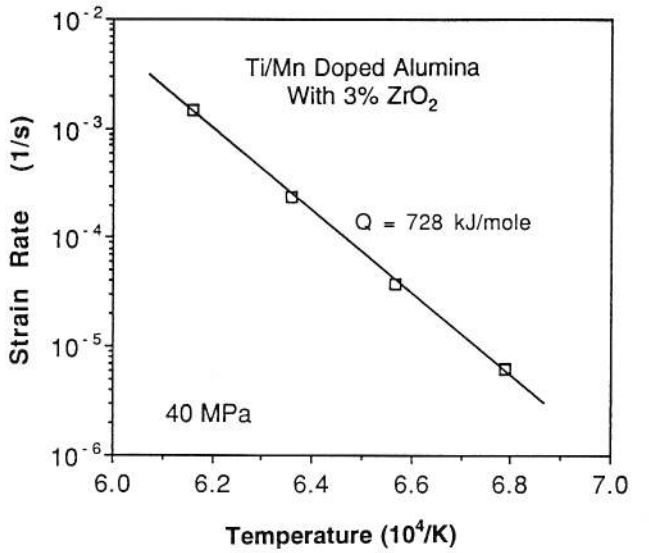

Fig. 5. Strain rate of the Ti/Mn-doped alumina with 3% ZrO_2 at 40 MPa as a function of reciprocal temperature.

(4) Postforming Annealing

After superplastic stretching, the 3-mol%-ZrO_2-added alumina still possessed a very fine microstructure with an average grain size of ~0.8 μm. To improve its high-temperature creep resistance we have attempted postforming annealing to coarsen the microstructure. After annealing at 1650°C for 4 h, the grain size increased to 23 μm, shown in Fig. 7. Most of the smaller zirconia particles had broken away from the alumina grain boundaries and were trapped within the grains.

The creep rate of the annealed alumina at 1400°C was measured and compared with that of the as-sintered one at 1350°C in Fig. 8. A large reduction is evident from these data despite the high deforming temperature of the annealed specimen. By extrapolating the data of the as-sintered specimen in Fig. 4 to 1400°C, we can see that annealing increases the creep resistance by a factor of 2000. The large difference in the deformation rate (2000 times) and the grain size (35 times) between the

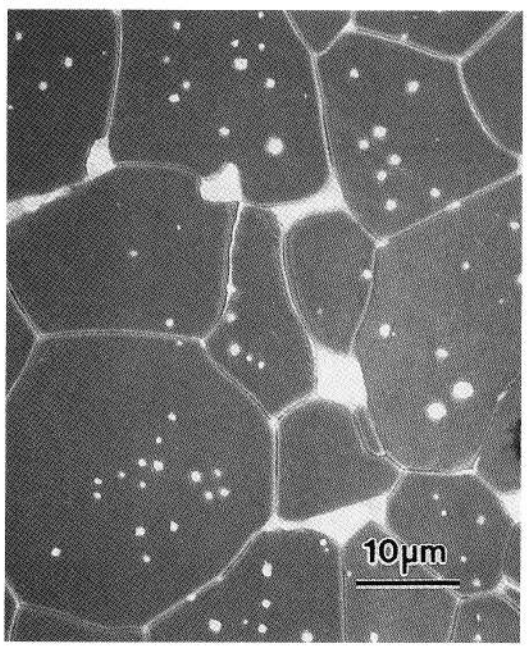

Fig. 7. SEM micrograph of a polished and thermally etched Ti/Mn-doped alumina specimen with intergranular and intragranular ZrO_2 particles (annealed at 1650°C for 4 h).

as-sintered and the annealed specimens also allows us to estimate the grain size exponent p. The value is 2.2, which is close to the one reported in the literature (~2).[3]

The distribution of Ti and Mn in the annealed material has been analyzed by EDX. As we mentioned earlier, in the as-sintered material the 1 mol% Mn concentration was below the detectability of the instrument. This was again the case for the annealed material which could be expected to have improved resolution and a stronger segregation due to the larger ZrO_2 and Al_2O_3 grain size. The enrichment of Ti in zirconia second phase, on the other hand, was evident. Using sintered mixtures of ZrO_2/TiO_2 as the standards, we found the average Ti concentration in ZrO_2 particles to be 5 mol%, i.e., an enrichment factor of 5. Since the balance of Ti concentration (0.85%) in alumina grains is still much higher than the solubility limit of Ti in Al_2O_3, this indirectly confirms that the codoping of Ti and Mn greatly increases the solubility of both ions.

IV. Discussion

The benefit of charge-compensating dopants to enhance the diffusion and deformation processes, to the extent of enabling low-temperature superplasticity in alumina, is established by the present study. The major features of deformation and microstructural characteristics are in agreement with the general understanding established for alumina and other fine-grained ceramics,[3] except for the mechanistic justification of the charge-compensating doping itself. The incorporation of Ti^{4+} or Mn^{2+}, separately, into alumina lattice can be described by the following defect equations:

$$3TiO_2 \rightarrow 3Ti_{Al}^{\cdot} + 6O_O + V_{Al}^{'''} \quad (2)$$

$$3MnO + Al_{Al} \rightarrow 3Mn_{Al}' + Al_i^{\cdot\cdot\cdot} \quad (3)$$

with respective charge neutrality conditions

$$3[V_{Al}^{'''}] = [Ti_{Al}^{\cdot}] \quad (4)$$

$$3[Al_i^{\cdot\cdot\cdot}] = Mn_{Al}^{\cdot}] \quad (5)$$

In either case, the Al defect concentration is increased proportionally to the dopant addition, so that the diffusion kinetics pertaining to sintering and deformation are enhanced as experimentally observed.[9–14] Since the defect formation energies in Al_2O_3 are quite high, the necessity of defect generation by aliovalent dopants also limits their solubility. The codoping of Ti with Mn, on the other hand, is thought to follow the self-compensating reaction:

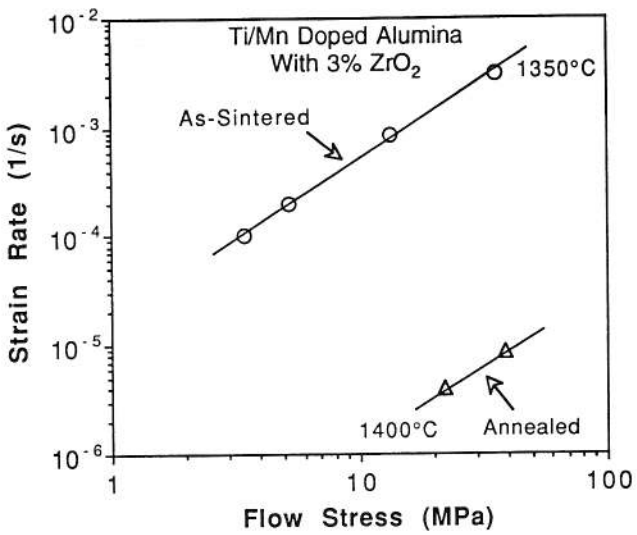

Fig. 8. Comparison of deformation rate for the Ti/Mn-doped alumina with 3% ZrO_2 before and after annealing.

$$TiO_2 + MnO \rightarrow Ti_{Al}^{\cdot} + Mn_{Al}^{\cdot} + 3O_O \quad (6)$$

Thus, large Al defect concentrations are no longer required; hence, the higher solubility for the two codopants in alumina.

The above simple argument suggests that enhanced solubility but not enhanced diffusivity is achieved by Ti and Mn codoping. (If charge compensation is not fully attained, because of incomplete ionization of Ti^{4+}/Ti^{3+} and Mn^{2+}/Mn^{3+} or unbalanced distribution of Ti/Mn, then enhanced diffusivity is possible but is limited to about the same extent achievable by a single dopant at its solubility limit.) The present and previous studies,[16–20] nevertheless, found that, over a very broad range of concentration, the charge-compensating dopants do significantly enhance the diffusion kinetics and that the enhancement increases with the dopant concentration. Although it might be suspected that,[19] with increasing Ti and Mn codoping, a large amount (e.g., 1–2%) of grain boundary liquid is formed, other evidence usually associated with the presence of liquid phase is lacking in the present system, as detailed below. First, microstructural examination by SEM did not reveal a second-phase coating along grain boundaries, and EDX point analysis did not detect any enrichment of Ti or Mn at the grain boundaries either. Second, differential thermal analysis (DTA) from room temperature to 1400°C did not find any endothermic peak. (In alumina doped with 2%-Cu-containing liquid phase, such a peak indicating liquid melting appeared at 1167°C.[34]) Third, deformation experiments did not find any apparent transition in either stress exponent or activation energy as the temperature rose. (Such a transition indicating a change of deformation mechanism from a solid-state one to a liquid-phase-assisted one as the melting point is exceeded was observed in 0.3–1-mol%-Cu-added 2Y-TZP,[24] 0.3 mol% Cu + 0.3 mol% Ti + 0.2 mol% B-added 2Y-TZP/alumina composite,[35] and in 2% Cu + Ti-added alumina.[4] Lastly, neither enhanced nor anisotropic grain growth was observed at higher sintering or annealing temperatures. (Large, strongly faceted, elongated, or platelike grains are commonly seen in liquid-containing alumina.[4,36,37]) Taken together, the above experimental evidence suggests that Ti and Mn codoping does not yield a large amount of liquid phase in the temperature range studied here.

An alternative rationalization for the enhanced kinetics is proposed using a modified defect picture allowing defect complexes. In this picture, the large concentrations of $V_{Al}^{'''}$ and $Al_i^{\cdot\cdot\cdot}$ due to doping are not entirely eliminated by recombination expected of the Frenkel pair. Instead, these defects are incorporated, as a result of Coulombic interactions between defects and dopants, into a variety of dopant–defect complexes, such as $(Mn_{Al}'Al_i^{\cdot\cdot\cdot})^{\cdot\cdot}$ $(2Mn_{Al}'Al_i^{\cdot\cdot\cdot})^{\cdot}$, $(Ti_{Al}^{\cdot}V_{Al}^{'''})''$, $(2Ti_{Al}^{\cdot}V_{Al}^{'''})'$, etc. A much higher solubility can then be maintained if these dopant–defect complexes, which are stabilized by electrostatic attractions, have lower energies than $V_{Al}^{'''}$ and $Al_i^{\cdot\cdot\cdot}$. Meanwhile, these associated defects can progressively dissociate locally at high temperatures to allow Al vacancies and interstitials to migrate between traps. Such traps are located at the appropriate aliovalent dopant sites, which are estimated to be spaced only five cations apart at a dopant concentration of 1 mol% (TiO_2·MnO). In this way, enhanced diffusion kinetics can indeed be anticipated upon addition of charge-compensating dopants at relatively large concentrations.

The above picture is not in violation of the basic thermodynamic expectation of the very low global concentrations of $V_{Al}^{'''}$ and $Al_i^{\cdot\cdot\cdot}$ at the test temperatures. Kinetically, an enhancement effect is always expected because of the higher defect concentrations at all temperatures. The enhancement is especially pronounced at higher temperatures because of more dissociation which in turn provides more "free" defects. Moreover, the temperature-dependent defect dissociation necessarily adds a contribution, of the order of association energy, to the observed activation energy of diffusion over the temperature range in which enhanced kinetics is apparent. This explains why the activation energy of the codoped, superplastic alumina is much higher than that for pure alumina. Note that the latter

observation of a higher activation energy and enhanced kinetics is not limited to Al_2O_3. For example, in Y_2O_3, we also found that Mg and Sr doping enhanced kinetics and increased activation energy, and conversely, Zr and Ce doping suppressed kinetics and decreased activation energy.[38] A similar model has also been constructed for apparent activation energies observed in the doped CeO_2 system.[39] Although further investigation is probably still needed, this picture of defect/dopant complexes seems capable of reconciling the salient features of charge-compensating doping.

V. Conclusions

(1) Charge-compensating aliovalent dopants, Ti^{4+} and Mn^{2+}, have a higher solubility in alumina and they significantly enhance the diffusion/deformation process during sintering and deformation. Codoping with 1 mol% Ti^{4+} and 1 mol% Mn^{2+} enhances the strain rate by at least a factor of 70.

(2) Static and dynamic grain growth in Ti and Mn-doped alumina can be brought under control by incorporating 3 mol% zirconia as a second-phase pinning agent.

(3) Through the above two approaches, a superplastic alumina has been obtained which can be shape-formed under biaxial tension to 100% strain at a temperature as low as 1280°C.

(4) The incorporation of charge-compensating dopants and the enhanced diffusion and increased activation energy it causes by that are rationalized by the formation and dissociation of dopant-defect complexes which are stabilized by Coulombic interactions.

References

[1]J. W. Edington, K. N. Melton, and C. P. Cutler, "Superplasticity," *Prog. Mater. Sci.*, **21** [2] 61–170 (1976).

[2]I-W. Chen and L. A. Xue, "Superplastic Alumina Ceramics with Grain Growth Inhibitors," *J. Am. Ceram. Soc.*, **73** [9] 2585–609 (1990).

[3]L. A. Xue, X. Wu, and I-W. Chen, "Development of Superplastic Structural Ceramics," *J. Am. Ceram. Soc.*, **74** [4] 842–45 (1991).

[4]L. A. Xue, "Effect of Liquid-forming Additives on Low-Temperature Superplastic Deformation of Alumina," *J. Mater. Sci. Lett.*, **11**, 1395–97 (1992).

[5]R. M. Cannon and R. L. Coble, "Review of Diffusional Creep of Al_2O_3"; pp. 61–100 in *Deformation of Ceramic Materials*. Edited by R. C. Bradt and R. E. Tressler. Plenum Press, New York, 1975.

[6]M. P. Harmer, "Use of Solid-Solution Additives in Ceramic Processing"; pp. 679–96 in Advances in Ceramics, Vol. 10, *Structure and Properties of MgO and Al_2O_3 Ceramics*. Edited by W. D. Kingery. American Ceramic Society, Columbus, OH, 1984.

[7]S. J. Bennison and M. P. Harmer, "Grain-Growth Kinetics for Alumina in the Absence of a Liquid Phase," *J. Am. Ceram. Soc.*, **68** [1] C-22–C-24 (1985).

[8]F. Wakai, T. Iga, and T. Nagano, "Effect of Dispersion of ZrO_2 Particles on Creep of Fine-Grained Al_2O_3," *J. Ceram. Soc. Jpn.*, **96** [12] 1206–209 (1988).

[9]R. D. Bagley, I. B. Cutler, and D. L. Johnson, "Effect of TiO_2 on Initial Sintering of Al_2O_3," *J. Am. Ceram. Soc.*, **53** [3] 136–41 (1970).

[10]R. J. Brook, "Effect of TiO_2 on the Initial Sintering of Al_2O_3," *J. Am. Ceram. Soc.*, **55** [2] C-114–C-115 (1972).

[11]J. R. Keski and I. B. Cutler, "Initial Sintering of Mn_xO–Al_2O_3," *J. Am. Ceram. Soc.*, **51** [8] 440–44 (1968).

[12]N. Kimura, S. Abe, J. Morishita, and H. Okamura, "Low-Temperature Sintering of Y-TZP and Y-TZP-Al_2O_3 Composites with Transition Metal Oxide Additives"; pp. 1142–48 in *Sintering 87*, Vol. 2. Edited by S. Somiya, M. Shimada, M. Yoshimura, and R. Watanabe. Elsevier Applied Science, New York, 1988.

[13]G. W. Hollenberg and R. S. Gordon, "Effect of Oxygen Partial Pressure on the Creep of Polycrystalline of Al_2O_3 Doped with Cr, Fe, or Ti," *J. Am. Ceram. Soc.*, **56** [3] 140–47 (1973).

[14]P. A. Lessing and R. S. Gordon, "Creep of Polycrystalline Alumina, Pure and Doped with Transition Metal Impurities," *J. Mater. Sci.*, **12**, 2291–302 (1977).

[15]R. K. Roy and R. L. Coble, "Solubilities of Magnesia, Titania, and Magnesium Titanate in Aluminum Oxide," *J. Am. Ceram. Soc.*, **51** [1] 1–6 (1968).

[16]I. B. Cutler, C. Bradshow, C. J. Christensen, and E. P. Hyatt, "Sintering of Alumina at Temperatures of 1400°C and Below," *J. Am. Ceram. Soc.*, **40** [4] 134–39 (1957).

[17]W. R. Cannon, "High Creep Ductility in Alumina Containing Compensating Additives"; pp. 741–49 in Advances in Ceramics, Vol. 10, *Structure and Properties of MgO and Al_2O_3 Ceramics*. Edited by W. D. Kingery. American Ceramic Society, Columbus, OH, 1984.

[18]Y. Ikuma and R. S. Gordon, "Effect of Doping Simultaneously with Iron and Titanium on the Diffusional Creep of Polycrystalline Al_2O_3," *J. Am. Ceram. Soc.*, **66** [2] 139–47 (1983).

[19]Y. Ikuma and R. S. Gordon, "Enhancement of the Diffusional Creep of Polycrystalline Al_2O_3 by Simultaneous Doping with Manganese and Titanium," *J. Mater. Sci.*, **17**, 2961–67 (1982).

[20]R. S. Gordon, "Understanding Defect Structure and Mass Transport in Polycrystalline Al_2O_3 and MgO via the Study of Diffusional Creep"; pp. 418–37 in Advances in Ceramics, Vol. 10, *Structure and Properties of MgO and Al_2O_3 Ceramics*. Edited by W. D. Kingery. American Ceramic Society, Columbus, OH, 1984.

[21]C. Carry and A. Mocellin, "Structural Superplasticity in Single Phase Crystalline Ceramics," *Ceramic. Int.*, **13**, 89–98 (1987).

[22]X. Wu and I-W. Chen, "Superplastic Bulging of Fine-Grained Zirconia," *J. Am. Ceram. Soc.*, **73** [3] 746–49 (1990).

[23]L. A. Xue and I-W. Chen, "Deformation and Grain Growth of Low-Temperature-Sintered High-Purity Alumina," *J. Am. Ceram. Soc.*, **73** [11] 3518–21 (1990).

[24]C-M. J. Hwang and I-W. Chen, "Effect of a Liquid Phase on Superplasticity of 2 mol%-Y_2O_3-Stabilized Tetragonal Zirconia Polycrystals," *J. Am. Ceram. Soc.*, **73** [6] 1626–32 (1990).

[25]L. W. Coughenour and R. S. Roth, "Phase Equilibrium Relations in the Systems Lime–Titania and Zirconia–Titania," *J. Res. Natl. Bur. Stand. (U.S.)*, **52**, 37 (1954).

[26]D. S. Wilkinson, "Grain Size Effects in Superplasticity"; Ch. 6, pp. 6.1–6.6 in *Superplasticity*. Edited by B. Baudelet and M. Suery. Centre National de la Recherche, Paris, France, 1985.

[27]K. R. Venkatachari and R. Raj, "Superplastic Flow in Fine-Grained Alumina," *J. Am. Ceram. Soc.*, **69** [2] 135–38 (1986).

[28]J. D. Fridez, C. Carry, and A. Mocellin, "Effects of Temperature and Stress on Grain Boundary Behavior in Fine-Grained Alumina"; pp. 720–40 in Advances in Ceramics, Vol. 10, *Structure and Properties of MgO and Al_2O_3 Ceramics*. Edited by W. D. Kingery, American Ceramic Society, Columbus, OH, 1984.

[29]R. M. Cannon, W. H. Rhodes, and A. H. Heuer, "Plastic Deformation of Fine-Grained Alumina (Al_2O_3). I. Interface-Controlled Diffusional Creep," *J. Am. Ceram. Soc.*, **63** [1–2] 46–53 (1980).

[30]A. H. Chokshi and J. R. Porter, "Higher Temperature Mechanical Properties of Single Phase Alumina," *J. Mater. Sci.*, **21**, 705–10 (1986).

[31]F. Wakai, Y. Kudama, S. Sakaguchi, N. Murayama, H. Kato, and T. Nagaro, "Superplasticity of ZrO_2/Al_2O_3 Duplex Composites"; pp. 259–66 in Proceedings of the MRS International Meeting on Advanced Materials, Vol. 7, *Superplastics*. Edited by M. Kobayashi and F. Wakai. Materials Research Society, Pittsburgh, PA, 1989.

[32]J. Wang and R. Raj, "Interface Effects in Superplastic Deformation of Alumina Containing Zirconia, Titanium and Hafnia as a Second Phase," *Acta Metall. Mater.*, **39** [11] 2909–19 (1991).

[33]J. Wang and R. Raj, "Estimation of the Activation Energies for Boundary Diffusion for Rate-Controlled Sintering of Pure Alumina in an Alumina Doped with Zirconia and Hafnia," *J. Am. Ceram. Soc.*, **73** [5] 1171–75 (1990).

[34]L. A. Xue and I-W. Chen, "Low-Temperature Sintering of Alumina with Liquid-Forming Additives," *J. Am. Ceram. Soc.*, **74** [8] 2011–13 (1991).

[35]L. A. Xue, "Enhanced Superplastic Deformation of 2 mol% Yttria-Stabilized Tetragonal Zirconia Polycrystals—Alumina Composite by Liquid-Forming Additives," *J. Mater. Sci. Lett.*, **10**, 1291–92 (1991).

[36]W. A. Kaysser, M. Sprissler, C. A. Handwerker, and J. E. Blendell, "Effect of a Liquid Phase on the Morphology of Grain Growth in Alumina," *J. Am. Ceram. Soc.*, **70** [5] 339–43 (1987).

[37]H. Song and R. L. Coble, "Origin and Growth Kinetics of Plate-like Abnormal Grains in Liquid-Phase-Sintered Alumina," *J. Am. Ceram. Soc.*, **73** [7] 2077–85 (1990).

[38]P. L. Chen, "CeO_2 and Y_2O_3 Systems—Powder Synthesis, Sintering, and Dopant Effects"; Ph.D. Thesis. Department of Materials Science and Engineering, University of Michigan, Ann Arbor, MI, 1995.

[39]P. L. Chen and I-W. Chen, "Role of Defect Interaction in Boundary Mobility and Cation Diffusivity of CeO_2," *J. Am. Ceram. Soc.*, **77** [9] 2289–97 (1994). □